Priority-based Coexistence of eMBB and URLLC Traffic in Industrial 5G NR Deployments

Ekaterina Markova[†], Dmitri Moltchanov[⋆], Rustam Pirmagomedov[⋆], Daria Ivanova[†],
Yevgeni Koucheryavy[⋆], and Konstantin Samouylov[†]
[†]RUDN University, Moscow, Russia
[⋆]Tampere University, Tampere, Finland.

***Abstract*—One of the most attractive use-cases for the 5G mobile cellular system is industrial automation. To this end, the newly standardized New Radio (NR) technology offers the support of both ultra-reliable low-latency (URLLC) service and conventional enhanced mobile broadband (eMBB) service. Owning to extreme latency and reliability requirements, URLLC service needs to be provided an explicit prioritization. We consider the simultaneous support of these two services in an industrial environment, where manufacturing machinery utilizes URLLC service for motion control and synchronous operation while eMBB service is used for remote monitoring. By utilizing the tools of stochastic geometry and queuing theory, we formalize the model with preemptive priority service at NR base stations (BS). The considered key performance indicator is the density of NR BS. Our numerical results indicate that the proposed approach does provide perfect isolation for URLLC traffic even in a dynamically changing environment and the required reliability level for a given load may indeed be attained by the proper selection of NR BS density and NR BS antenna arrays.**

I. Introduction

The fifth-generation mobile systems being standardized by 3GPP, are expected to appear on the industrial automation market in the near future [1]. In industrial automation scenarios, 5G NR promises new applications, such as the joint operation of mobile robots, wireless time synchronization, positioning, augmented reality services for personnel, and telepresence-based maintenance operations. The systems that control the moving elements of manufacturing equipment commonly generate low-rate traffic but require ultra-reliable low-latency service (URLLC). Meanwhile, video-guided machinery or mobile robots require enhanced mobile broadband (eMBB) service. Thus, NR BSs need to support a mixture of eMBB and URLLC services at the same time.

There have only been a few approaches considered in recent literature to enable coexistence between URLLC and eMBB while still preserving the strict requirements of the former. In [2], the authors advocate using the non-orthogonal multiple access (NOMA) technology at the air interface for providing URLLC transmissions with the eMBB ones in case of overloaded conditions. One of the inherent advantages of this approach is that URLLC data can be immediately scheduled without waiting until the end of the current NR frame for conventional scheduling. However, this approach affects eMBB traffic and required careful selection of eMBB sections to be affected. The authors in [3] studied the process of joint scheduling of the considered services at a single NR BS by solving the associated optimization problem. However, larger deployments were not addressed.

Another viable option for simultaneous support of the considered traffic types relies on the explicit resource reservation for URLLC traffic [4]. As the load of URLLC traffic is unknown in advance, a prediction mechanism is required to update the allocated resources, respectively [5], [6]. As these allocations can be updated only at a NR frame time instance, the latency requirement of URLLC data may not be met. A similar effect can be achieved by prioritizing URLLC traffic over eMBB. Here, when a load of URLLC traffic increases such that there are insufficient resources to transmit it, one or more eMBB sessions might be dropped. To the best of our knowledge, there are no studies elaborating on this approach.

In this paper, we endeavor to enable the simultaneous support of eMBB and URRLC services via an explicit prioritization method and provide a model for assessing the mmWave BS density required for that. To this aim, we combine the tools of stochastic geometry and queuing theory to build a performance evaluation framework that captures mmWave-specific propagation at the air interface and session service dynamics on mmWave BS. The main metric of interest is the density of BSs required to support a given intensity of URLLC and eMBB sessions with the prescribed performance guarantees. The latter is specified in terms of session drop probabilities and system resource utilization that serve as intermediate metrics. The main contributions of our study are:

- performance evaluation framework for assessing the required density of mmWave BSs with explicit prioritization of URLLC traffic in the presence of eMBB traffic;
- the proposed approach provides isolation for URLLC traffic, and the loss level of 10^{-6} for a given load may indeed be attained by proper selection of NR BS density and NR BS antenna arrays.

The paper is organized as follows. We review the scope and applications of 5G NR in industrial automation in Section II. Further, in Section III we introduce our system model. In Section IV we formalize our performance evaluation framework. Numerical results are elaborated in Section V, and conclusions are drawn in the final section.

II. 5G NR in Industrial Environment

The 5G NR technology promises a wireless network enabling multiple innovative applications, including Industry 4.0. The 5G systems rely upon a completely novel architecture

with explicitly separated user and control planes and combine different frequency bands covering specific services, including mMTC, URRLC, eMBB. User equipment (UE) in NR is capable of selecting the required bandwidth dynamically depending on their current needs by switching between the configured Bandwidth Parts (BWP). Up to four different BWPs can be configured simultaneously for a UE; however only one can be active at a moment in time. This allows one network to serve applications with different requirements while ensuring the efficient use of radio resources.

According to [7], the main niches for 5G-enabled wireless connectivity in an industrial environment include the following domains: (i) replacement of wired connections used by legacy equipment, (ii) motion control and control-to-control communication, (iii) mobile robotic platforms, (iv) processes monitoring. Wireless connectivity should replace legacy technologies that are currently dominating at the operational technology level, e.g., PROFINET, EtherCAT, Sercos, Modbus [8]. This objective is critically important for reducing costs at the earliest stage of the transformation towards Industry 4.0 when legacy manufacturing machines should be seamlessly integrated into the emerging wireless deployment.

A mobile robotic platform is an essential tool for automation on the factory floor. Such devices are autonomously guided and may perform a variety of technological operations [9]. Their operation relies upon real-time communication between sensors scanning the environment, actuators, and a motion controller. The control-to-control communications enabling coordination between different industrial controllers is more relaxed compared to motion control in terms of latency requirements. However, control-to-control data varies in size and periodicity, which result in dynamically changing traffic demands at the air interface.

Expectedly, personnel will still continue to play a substantial role in future smart factories [7]. Interaction between people and machines can be enabled by a wide set of interfaces. Conventional control and operation panels are expected to further evolved towards full mobility support of a human user. In addition to those, manufacturing processes are expected to benefit from using Augmented Reality (AR) technologies. The AR-based devices with head-mounted see-through displays may facilitate guidance and ad hoc support for workers on the floor, empowering smooth operation and efficient human-machine cooperation. Depending on the particular deployment, the aggregated data flow may reach several Gbps requiring extremely high capacity at the air interface.

III. System Model

1) Deployment: We consider a private 5G NR deployment in an industrial environment, e.g., a large autonomous factory with multiple production lines, as illustrated in Fig. 1. We assume that NR BSs follow the Poisson point process (PPP) in $\Re^2$ with density χ BS/m^2. NR BSs are assumed to be mounted on the ceiling at the same height h_A. The operational bandwidth at each NR BS is W.

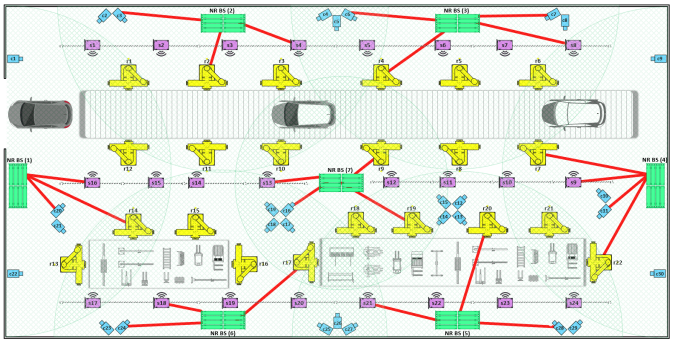

Fig. 1. The considered autonomous factory deployment.

There are two types of UEs, motion control devices (e.g., sensors, actuators) and monitoring units (e.g., cameras). Motion control devices are associated with robotized equipment or production lines and they generate URLLC traffic that requires both uplink and downlink transmissions. The monitoring units, represented by video cameras, generate eMBB traffic and utilize uplink only. The uplink and downlink are assumed to be separated in time. We concentrate on an uplink direction, assuming that a downlink has sufficient resources to immediately send sensory traffic as there is no monitoring traffic in that direction. The geographical locations of sensors and monitoring UEs are assumed to follow PPPs as well.

2) Propagation and Antenna Models: The signal-to-noise plus interference ratio (SINR) at the receiver located at the distance of y from the NR BS is given by

$$S(y) = \frac{P_U G_A G_U}{N_0 W L(y) M_I M_S}, \tag{1}$$

where P_U is the UE transmit power, G_A and G_U are the antenna array gains at the NR and the UE ends, respectively, N_0 is the power spectral density of noise, W is the operating bandwidth, $L(y)$ is the linear path loss, M_I is the interference margin, and M_S is the shadow fading margin.

We capture any interference from the adjacent NR BSs via an interference margin M_I. For a given NR BS deployment density, one may estimate it precisely by employing stochastic geometry based models [10]–[12]. The effect of shadow fading is accounted for by using the shadow fading margin, M_S [13].

Following [13], the path loss measured in dB is given by

$$L_{dB}(y) = 32.4 + 21 \log_{10} y + 20 \log_{10} f_c, \tag{2}$$

where f_c is the operating frequency in GHz and y is the three-dimensional (3D) distance between the NR AP and the UE.

The path loss in the form of (2) can be represented in the linear scale by utilizing the model in the form of $Ay^{-\zeta}$, where ζ_1, ζ_2 are propagation are the propagation coefficients in line-of-sight (LoS) and non-LoS states, respectively, i.e.,

$$A = 10^{2 \log_{10} f_c + 3.24} M_S M_I, \; \zeta_1 = 2.1, \; \zeta_2 = 3.18. \tag{4}$$

The value of SNR at the UE can then be written as

$$S(y) = C y^{-\zeta}, \tag{5}$$

where $C = P_U G_A G_U / (N_0 W A M_I M_S)$,

$$[\lambda_1 I\{n_1 < N_1, b_1(n_1+1) + b_2^{\min} n_2 \le C\} + \lambda_2 I\{n_2 < N_2, b_1 n_1 + b_2^{\min}(n_2+1) \le C\} + n_1\mu_1 + n_2\mu_2 +$$
$$+ \lambda_1 I\{n_1 < N_1, n_2 > 0, b_1(n_1+1) + b_2^{\min} n_2 > C\}]p(n_1,n_2) = \lambda_1 I\{n_1 > 0, b_1 n_1 + b_2^{\min} n_2 \le C\}p(n_1-1,n_2) +$$
$$+ \lambda_2 I\{n_2 > 0, b_1 n_1 + b_2^{\min} n_2 \le C\}p(n_1,n_2-1) + (n_1+1)\mu_1 I\{n_1 < N_1, b_1(n_1+1) + b_2^{\min} n_2 \le C\}p(n_1+1,n_2) +$$
$$+ (n_2+1)\mu_2 I\{n_2 < N_2, b_1 n_1 + b_2^{\min}(n_2+1) \le C\}p(n_1,n_2+1) +$$
$$+ \lambda_1 I\{n_1 > 0, n_2+1 \le N_2, b_1(n_1-1) + b_2^{\min}(n_2+1) \le C, b_1 n_1 + b_2^{\min}(n_2+1) > C\}p(n_1-1,n_2+1) + ... +$$
$$+ \lambda_1 I\{n_1 > 0, b_1(n_1-1) + b_2^{\min} k(n_1-1) \le C, b_1 n_1 + b_2^{\min} k(n_1-1) > C\}p(n_1-1, k(n_1-1)). \quad (3)$$

Following [11], [14], we assume a cone antenna model with the radiation pattern represented by a conical zone with an angle of α coinciding with the HPBW. The latter is proportional to the number of antenna elements as [15]

$$\alpha = 2|\theta_m - \theta_{3db}|, \quad (6)$$

where θ_{3db} is the 3dB angle and θ_m is the array maximum.

The mean antenna gain over the HPBW can be found as [15]

$$G = \frac{1}{\theta_{3db}^+ - \theta_{3db}^-} \int_{\theta_{3db}^-}^{\theta_{3db}^+} \frac{\sin(N\pi\cos(\theta)/2)}{\sin(\pi\cos(\theta)/2)} d\theta, \quad (7)$$

where the upper and the lower 3-dB points are

$$\theta_{3db}^{\pm} = \arccos[-\beta \pm 2.782/(N\pi)], \quad (8)$$

and N is the number of antenna elements.

3) Traffic and Resource Allocation: The arrival of monitoring sessions is assumed to form Poisson process with intensity λ_M. These sessions generate elastic traffic with minimum rate requirements $c_2^{\min}$, $c_2^{\min} \ge 1$. In practice, elasticity implies that the end application may change the codec rate to adapt to the current network conditions but there is a minimum floor – $c_2^{\min}$. The loss of these sessions may happen at the moment of arrival or during the service. The session service time is exponentially distributed with the mean μ_M^{-1}.

Sensor traffic is assumed to arrive according to Poisson process with intensity λ_S. Rate requirements are static, c_1, $c_1^{\min} \ge 1$, but resource requirements may vary depending on UE location. Similarly to [3], the value of c_1 is determined based on the data rate and the required level of reliability, 10^{-6} BLER for URLLC, assuming replication coding. The loss of these sessions may only happen at the moment of arrival when all system resources are busy with other sensor traffic. The service time is exponentially distributed with the mean μ_S^{-1}.

Since URLLC sensory sessions are latency-critical we assume that they are provided exclusive access to the transmission resources via preemptive-priority service discipline. Particularly, if there is a lack of resources to serve URLLC sessions, one or more eMBB sessions can be interrupted. URLLC sessions can only be lost if their aggregated instantaneous load exceeds the system transmission resources.

4) Metrics of Interest: We concentrate on determining the density of NR BS for a given intensity of UEs such that the prescribed guarantees are met. These guarantees are specified in terms of session drop probabilities of both traffic classes as well as resource utilization of the system.

IV. Performance Evaluation Model

A. Queuing Model

Taking into account that the arrival processes are Poisson in nature while service times are exponentially distributed the behavior of the NR BS serving URLLC and eMBB traffic can be approximated by a two-dimensional continuous-time Markov chain (CTMC) $\mathbf{X}(t) = \{N_1(t), N_2(t), t > 0\}$, where $N_1(t)$ is the number of URLLC sessions, $N_2(t)$ is the number of eMBB sessions at the time instant t. The state-space of the CTMC $\mathbf{X}(t)$ is given by

$$\mathbf{X} = \{(n_1,n_2) : n_1 \ge 0, n_2 \ge 0, n_1 b_1 + n_2 b_2^{\min} \le C\}, \quad (10)$$

where n_1 is the current number of served URLLC sessions, n_2 is the current number of served eMBB sessions.

Let us introduce the following notations: (i) $N_1 = \lfloor C/b_1 \rfloor$ – maximum number of URLLC sessions in service, (ii) $N_2 = \lfloor C/b_2^{\min} \rfloor$ – the maximum number of eMBB sessions in service, $k(n_1) = \lfloor C - n_1 b_1/b_2^{\min} \rfloor$ – the maximum number of eMBB sessions, that can be in service when the current number of URLLC sessions in the system is n_1. Due to the elastic nature of eMBB sessions, characterized by uniform distribution of the channel rate between all the simultaneously served eMBB sessions, the achievable bitrate $b_2(n_1,n_2)$ for this type of sessions depends on the state $(n_1,n_2) \in \mathbf{X}$ of the system and is determined as

$$b_2(n_1,n_2) = \left\lfloor \frac{C - n_1 b_1}{n_2} \right\rfloor \ge b_2^{\min}. \quad (11)$$

To understand the operation of the system, consider admission control procedure, first, from the standpoint of the URLLC sessions, and, second, from the standpoint of the eMBB sessions. When a new URLLC session arrives to the system, three cases are possible:

- when the arriving session finds the system having greater than or equal to b_1 PRBs free the session is accepted and no eMBB sessions are preempted (dropped);
- when the following conditions are simultaneously satisfied at the moment of session arrival: (i) there are less than b_1 PRBs free, (ii) the number of URLLC sessions is less than N_1, and (iii) the current number of served eMBB sessions is greater than 0, the arriving session is accepted and exactly $\lceil (b_1 - C + (n_1 b_1 + n_2 b_2^{\min}))/b_2^{\min} \rceil$ eMBB sessions are simultaneously preempted;
- otherwise, the arriving URLLC session is dropped.

For a newly arriving eMBB session the following applies:

$$a((n_1,n_2),(n_1',n_2')) = \begin{cases} \lambda_1, & \text{if } n_1' = n_1+1, n_2' = n_2, n_1 < N_1, b_1(n_1+1) + b_2^{\min} n_2 \le C, \\ & \text{or } n_1' = n_1+1, n_2' = n_2 - l(n_1,n_2), n_1 < N_1, n_2 > 0, b_1(n_1+1) + b_2^{\min} n_2 > C; \\ \lambda_2, & \text{if } n_1' = n_1, n_2' = n_2+1, n_2 < N_2, b_1 n_1 + b_2^{\min}(n_2+1) \le C; \\ n_1\mu_1, & \text{if } n_1' = n_1-1, n_2' = n_2, n_1 > 0; \\ n_2\mu_2, & \text{if } n_1' = n_1, n_2' = n_2-1, n_2 > 0; \\ *, & \text{if } n_1' = n_1, n_2' = n_2; \\ 0, & \text{otherwise.} \end{cases} \tag{9}$$

- when the arriving session finds the system having greater than or equal to $b_2(n_1,n_2)$ PRBs free, it is accepted to the system and provided the bitrate $b_2(n_1,n_2)$;
- otherwise, the arriving eMBB session is dropped.

Using the formulated rules one may specify the state transition diagram of the defined CTMC model $\mathbf{X}(t)$ as illustrated in Fig. 2. Applying the local balance principle to the diagram, we derive the equilibrium equations as in (3) for $n_1 = 0,1,\ldots,N_1$ and $n_2 = 0,1,\ldots,N_2$ regulating transition rates in the considered model, where we denote

$$\left\lceil \frac{b_1 - C + (n_1 b_1 + n_2 b_2^{\min})}{b_2^{\min}} \right\rceil = l(n_1,n_2). \tag{12}$$

Let $(p(n_1,n_2))_{(n_1,n_2)\in\mathbf{X}} = \mathbf{p}$ be the stationary state probability distribution of CTMC $\mathbf{X}(t)$. As a result of preemptive-priority service mechanism, the considered Markov chain is not a reversible, implying that the stationary state probability distribution $p(n_1,n_2),(n_1,n_2) \in \mathbf{X}$ does not have product form solution. However, one can determine it numerically. For this purpose, we rewrite the system (3) as

$$\mathbf{pA} = \mathbf{0}, \mathbf{p1}^{\boldsymbol{T}} = 1, \tag{13}$$

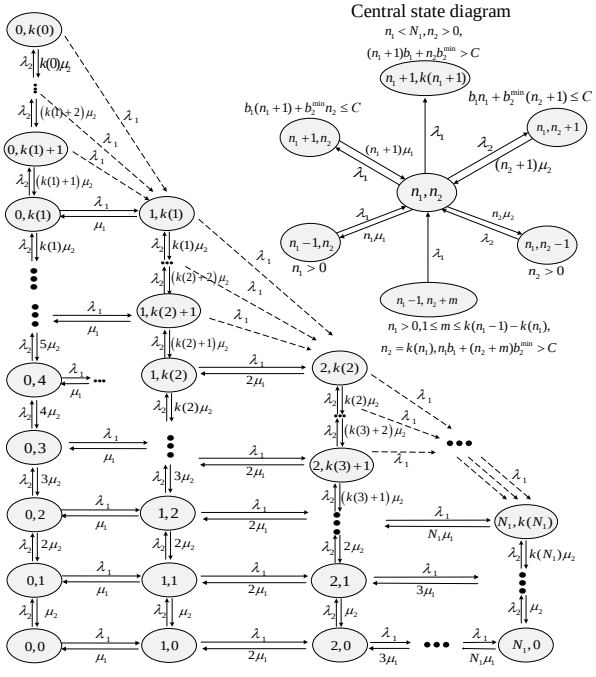

Fig. 2. The general view of the state transition diagram.

where $\mathbf{A}$ is the generator whose elements $a((n_1,n_2),(n_1',n_2'))$ are defined as (9), with the shorthand notation

$$\begin{aligned} * = -[&\lambda_1 I\{n_1 < N_1, b_1(n_1+1) + b_2^{\min} n_2 \le C\} + \\ &+ \lambda_1 I\{n_1 < N_1, n_2 > 0, b_1(n_1+1) + b_2^{\min} n_2 > C\} + \\ &+ \lambda_2 I\{n_2 < N_2, b_1 n_1 + b_2^{\min}(n_2+1) \le C\} + \\ &+ n_1\mu_1 + n_2\mu_2]. \end{aligned} \tag{14}$$

Having found the stationary state probability distribution $p(n_1,n_2),(n_1,n_2) \in \mathbf{X}$, one can compute the performance measures of the considered system as follows:

- URLLC session drop probability,

$$B_1 = \sum_{i=0}^{k(N_1)} p(N_1,i). \tag{15}$$

- eMBB session drop probability,

$$B_2 = \sum_{i=0}^{N_1} p(i,k(i)). \tag{16}$$

- eMBB session preemption probability Π, i.e., the probability that an arbitrary eMBB session served in the system is dropped during the service is given by

$$\Pi = \sum_{i=0}^{N_1-1} \sum_{\substack{j=k(i+1)+1 \\ k(i)\neq k(i+1)}}^{k(i)} \frac{\lambda_1 p(i,j)}{\lambda_1 + \lambda_2 I\{j < k(i)\} + i\mu_1 + j\mu_2}. \tag{17}$$

- resource utilization rate U, is given by

$$U = C\sum_{i=0}^{N_1}\sum_{j=1}^{k(i)}(i+j)p(i,j) + b_1\sum_{i=1}^{N_1} i p(i,0). \tag{18}$$

B. Model Parameterization

To parameterize the queuing system modeling the service process at NR BS we need to provide the amount of resources required to maintain minimum rate of eMBB and URLLC sessions, $b_2^{\min}$ and b_1, respectively. To determine the sought parameters we need to first characterize the effective coverage radii of NR BS, r_N. Observe that in the Poisson field of NR BSs the effective coverage radius r_N is determined by the interplay between the distance between NR BS, $r_{N,V}$, and maximum coverage of a NR BS, $r_{N,S}$. Thus, we have $r_N = \min(r_{N,S}, r_{N,V})$. Below we determine $r_{N,S}$ and $r_{N,V}$.

The radius $r_{N,S}$ is defined as the maximum separation between the UE and the NR BS, such that the UE in the LoS

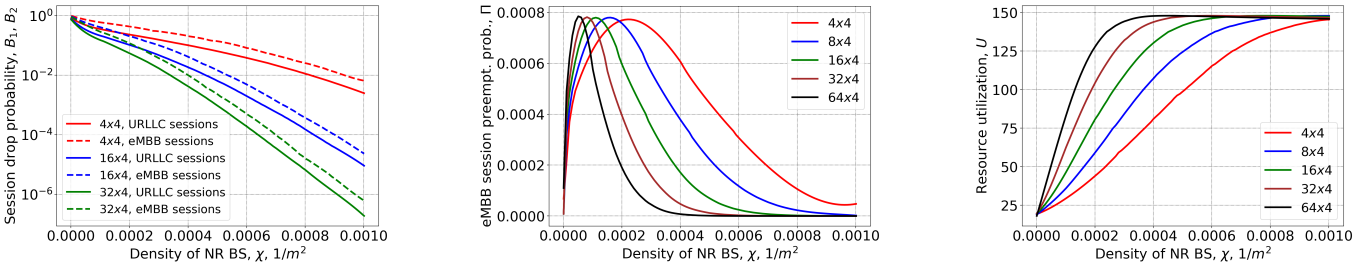

(a) Drop probability (b) Preemption probability (c) Utilization

Fig. 3. System performance metrics, $c_2^{\min} = 12.5$ Mbps, $\mu^{-1} = 120$ s.

blocked conditions is not in outage conditions. According to our propagation model, the SNR at the 2D distance $r_{N,S}$ is

$$S = C\left(r_{N,S}^2 + (h_A - h_U)^2\right)^{-\frac{\zeta}{2}} = S_{th}, \tag{19}$$

where S_{th} is the SNR corresponding to the lowest feasible NR MCS [16]. Solving this equation for d_N, we obtain

$$r_{N,S} = \sqrt{(C/S_{th})^{\frac{2}{\zeta}} - (h_A - h_U)^2}. \tag{20}$$

Note that $r_{N,S}$ depends on C in (5), which, in its turn, depends on the sector angle α according to (6)–(7). We approximate the radius $r_{N,V}$, characterizing the half distance between NR BS locations, by circle approximation of the Voronoi cell induced by NR BS locations in $\Re^2$. Since the actual area of Voronoi cell is not known [17] we utilize computer simulations to obtain $r_{N,V}$.

Once radii r_N and r_S are obtained, one may proceed characterizing the requires resources, $b_{\min}$ and b_S. Recalling that UEs are assumed to follow PPP in $\Re^2$ for NR part of NR BS the mean spectral efficiency can be obtained as follows

$$E[S_e] = \int_0^{r_N} \frac{2x}{r_N} \log_2(1 + S(y))dx, \tag{21}$$

where $S(y)$ is defined in (5).

Accounting for the rate of applications and available bandwidth at NR BS, W, one may now use the mean spectral efficiency to the mean amount of resources requested by UE as $b_2^{\min} = c_2^{\min}/E[S_e]$ and $b_1 = c_1/E[S_e]$.

TABLE I
PARAMETERS UTILIZED FOR NUMERICAL ASSESSMENT.

Parameter	**Value**
Carrier frequency	28 GHz
NR BS bandwidth	50 MHz
Transmit power	0.2 W
NR BS side antenna array	4x4, 8x4, 16x4, 32x4, 64x4
UE side antenna array	4x4
NR BS and UE heights	6 m, 1 m
Arrival intensity of URLLC sessions	0.114
Arrival intensity of eMBB sessions	0.0005
Mean service time of URLLC sessions	1 ms
Mean service time of eMBB sessions	120 s, 6000 s
Rate of URLLC sessions	2 Mbps
Minimum rate of eMBB sessions	12,5 Mbps, 25 Mbps

V. Numerical Results

Numerical results reported in this section were obtained for the system parameters shown in Table I. To approximate URLLC traffic transmission latency we set the associated mean service time to NR frame duration, 1 ms. To ensure reliable delivery of data within this deadline we assume repetition coding, i.e., the same replica of the URLLC message is repeated three times within the same NR frame. The rate of URLLC session in Table I is computed accounting for these overheads and assuming transmission of 80 bytes of payload.

We start the analysis with Fig. 3 that shows eMBB session drop and preemption probabilities, URLLC session drop probability, and system resource utilization as a function of NR BS density χ for minimum monitoring session rate of $c_2^{\min} = 12.5$ Mbps and duration of 120 s and different antenna arrays at NR BS. The plots indicate that the increase in NR BS density leads to a nearly exponential decrease in associated session drop probabilities. However, for the considered parameters the intended region of URLLC session drop probabilities of 10^{-6} is only attained at extreme NR BS densities of 0.0008 BS/m^2 for 32×4 antennas. The eMBB session preemption probability decreases as NR BS are more densely deployed implying that guaranteeing URLLC we also drastically improve monitoring session performance. Finally, we note that using of a 64×4 antenna array provides the best resource utilization advocating for advanced antenna solutions at NR BSs.

We now proceed with illustrating the system response to higher service time and the minimum rate of monitoring sessions, set to 6000 s and 25 Mbps, respectively, shown in Fig. 4 as a function of NR BS density χ for different antenna arrays at NR BS. In our context, such extreme service times capture the always-on operation of monitoring cameras. Comparing the presented results to those of Fig. 3, we notice that URLLC traffic performance is completely independent of the eMBB, which is a direct consequence of employed preemptive-priority service discipline. Analyzing the behavior of monitoring the eMBB session preemption probabilities, we note that it increases almost two times across the whole considered range of NR BS density, χ. This effect is a consequence of the higher load imposed by eMBB sessions. The resource utilization results remain qualitatively similar to those illustrated in Fig. 3.

Finally, we illustrate the considered metrics as a function of URLLC arrivals intensity λ_1 in Fig. 5, for three selected

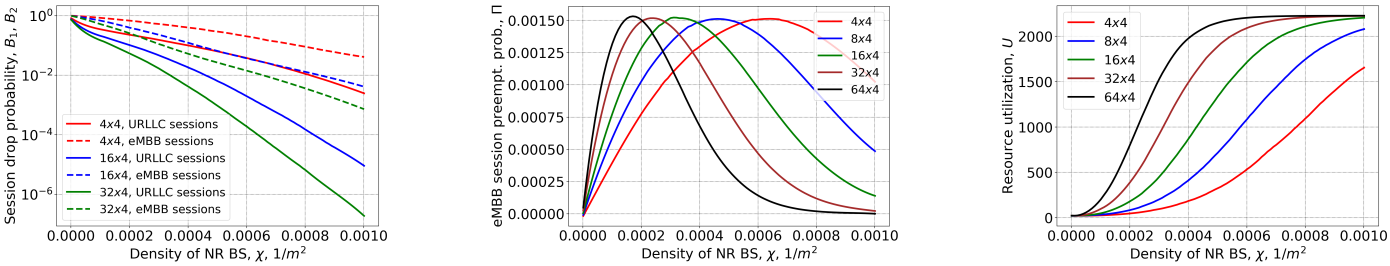

(a) Drop probability (b) Preemption probability (c) Utilization

Fig. 4. System performance metrics, $c_2^{\min} = 25$ Mbps, $\mu^{-1} = 6000$ s.

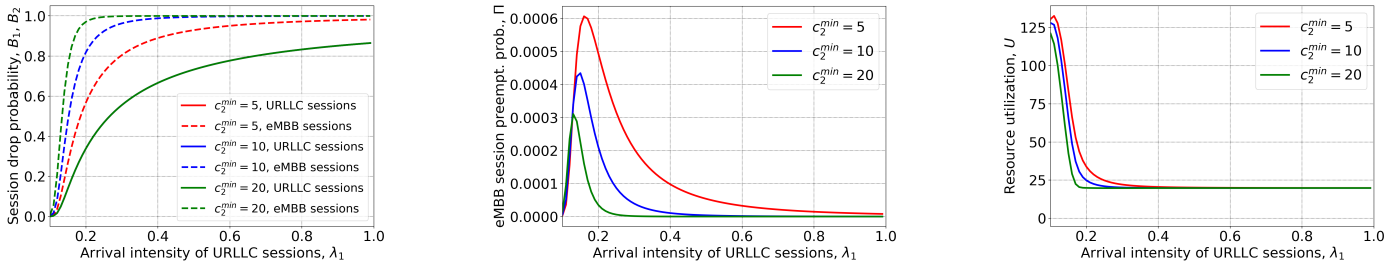

(a) Drop probability (b) Preemption probability (c) Utilization

Fig. 5. System performance metrics, NR BS array 16×4, NR BS density $\chi = 0.0005$ 1/m^2, $\mu^{-1} = 120$ s.

minimum rates of eMBB sessions, NR BS density $\chi = 0.0005$, NR BS antenna 16×4 and $\mu_2 = 1/120$. As one may observe the increase in λ_1 only mildly affects the URLLC session drop probability while the effect on eMBB preemption and drop probability is drastic.

VI. Conclusions

In this paper, we proposed the explicit prioritization technique for the improvement of URLLC services in industrial deployments of 5G NR. To characterize the gains of the proposed solution, we developed an analytical model which allows for capturing the service process of the mixture of eMBB and URLLC traffic with the preemptive-priority service order. The KPI of interest is the density of NR BS needed for serving the mixture of eMBB and URLLC traffic with prescribed performance guarantees. This density is determined numerically based on individual traffic performance metrics and system resource utilization.

Our numerical results indicate that the proposed approach does provide perfect isolation for URLLC traffic even in a dynamically changing environment, where the characteristic of eMBB traffic may dynamically shift. Furthermore, the maximum loss level of 10^{-6} may indeed be attained in dense deployment with advanced antenna arrays at NR BS. Particular values of NR BS density, satisfying given performance guarantees for selected system and traffic parameters, can be evaluated using the provided dependencies.

References

[1] A. Ghosh, R. Ratasuk, and A. M. Rao, "Industrial IoT Networks Powered by 5G New Radio," *Microwave Journal*, vol. 62, no. 12, 2019.

[2] R. Kassab et. al, "Coexistence of URLLC and eMBB services in the C-RAN uplink: an information-theoretic study," in *2018 IEEE Global Communications Conference (GLOBECOM)*. IEEE, 2018, pp. 1–6.

[3] A. Anand et. al, "Joint scheduling of urllc and embb traffic in 5g wireless networks," *IEEE/ACM Transactions on Networking*, 2020.

[4] P. Popovski, K. F. Trillingsgaard, O. Simeone, and G. Durisi, "5G wireless network slicing for eMBB, URLLC, and mMTC: A communication-theoretic view," *IEEE Access*, vol. 6, pp. 55 765–55 779, 2018.

[5] J. Park and M. Bennis, "URLLC-eMBB slicing to support VR multimodal perceptions over wireless cellular systems," in *2018 IEEE Global Communications Conference (GLOBECOM)*. IEEE, 2018, pp. 1–7.

[6] M. Alsenwi, N. H. Tran, M. Bennis, A. K. Bairagi, and C. S. Hong, "eMBB-URLLC resource slicing: A risk-sensitive approach," *IEEE Communications Letters*, vol. 23, no. 4, pp. 740–743, 2019.

[7] 3GPP, "Service requirements for cyber-physical control applications in vertical domains," TS 22.104 V17.2.0, Dec 2019.

[8] J. Sachs, K. Wallstedt, F. Alriksson, and G. Eneroth, "Boosting smart manufacturing with 5g wireless connectivity," *Ericsson Tech. Rev*, 2019.

[9] H. Kagermann, W. Wahlster, and J. Helbig, "Recommendations for implementing the strategic initiative industrie 4.0: Final report of the industrie 4.0 working group," *Acatech, München*, pp. 19–26, 2013.

[10] R. Kovalchukov, D. Moltchanov, A. Samuylov, A. Ometov, S. Andreev, Y. Koucheryavy, and K. Samouylov, "Analyzing effects of directionality and random heights in drone-based mmwave communication," *IEEE Transactions on Vehicular Technology*, vol. 67, no. 10, pp. 10 064–10 069, 2018.

[11] V. Petrov, M. Komarov, D. Moltchanov, J. M. Jornet, and Y. Koucheryavy, "Interference and SINR in Millimeter Wave and Terahertz Communication Systems With Blocking and Directional Antennas," *IEEE Trans. on Wirel. Comm.*, vol. 16, no. 3, pp. 1791–1808, 2017.

[12] R. Kovalchukov, D. Moltchanov, A. Samuylov, A. Ometov, S. Andreev, Y. Koucheryavy, and K. Samouylov, "Evaluating sir in 3d millimeter-wave deployments: Direct modeling and feasible approximations," *IEEE Transactions on Wireless Communications*, vol. 18, no. 2, pp. 879–896, 2018.

[13] 3GPP, "Study on channel model for frequencies from 0.5 to 100 GHz (Release 14)," 3GPP TR 38.901 V14.1.1, July 2017.

[14] V. Petrov, D. Moltchanov, and Y. Koucheryavy, "Interference and sinr in dense terahertz networks," in *2015 IEEE 82nd Vehicular Technology Conference (VTC2015-Fall)*. IEEE, 2015, pp. 1–5.

[15] A. B. Constantine *et al.*, "Antenna theory: analysis and design," *Microstrip Antennas (third edition), John Wiley & Sons*, 2005.

[16] 3GPP, "NR; Physical channels and modulation (Release 15)," 3GPP TR 38.211, Dec 2017.

[17] M. Tanemura, "Statistical distributions of Poisson Voronoi cells in two and three dimensions," *FORMA*, vol. 18, no. 4, pp. 221–247, 2003.